UCLA
UCLA Previously Published Works

Title

Obstructive sleep apnea is associated with altered midbrain chemical concentrations.

Permalink

https://escholarship.org/uc/item/0tk0t55m

Authors

Macey, Paul M

Sarma, Manoj K

Prasad, Janani P

et al.

Publication Date

2017-11-01

DOI

10.1016/j.neuroscience.2017.09.001

Peer reviewed

OBSTRUCTIVE SLEEP APNEA IS ASSOCIATED WITH ALTERED MIDBRAIN CHEMICAL CONCENTRATIONS

PAUL M. MACEY, [a,b*] MANOJ K. SARMA, [c]
JANANI P. PRASAD, [a] JENNIFER A. OGREN, [e]
RAVI AYSOLA, [d] RONALD M. HARPER [b,e] AND M. ALBERT
THOMAS [c]

[a] *School of Nursing, David Geffen School of Medicine at UCLA, University of California at Los Angeles, Los Angeles, CA 90095, United States*

[b] *Brain Research Institute, David Geffen School of Medicine at UCLA, University of California at Los Angeles, Los Angeles, CA 90095, United States*

[c] *Department of Radiological Sciences, David Geffen School of Medicine at UCLA, University of California at Los Angeles, Los Angeles, CA 90095, United States*

[d] *Department of Medicine (Division of Pulmonary and Critical Care), David Geffen School of Medicine at UCLA, University of California at Los Angeles, Los Angeles, CA 90095, United States*

[e] *Department of Neurobiology, David Geffen School of Medicine at UCLA, University of California at Los Angeles, Los Angeles, CA 90095, United States*

Abstract—Obstructive sleep apnea (OSA) is accompanied by altered structure and function in cortical, limbic, brainstem, and cerebellar regions. The midbrain is relatively unexamined, but contains many integrative nuclei which mediate physiological functions that are disrupted in OSA. We therefore assessed the chemistry of the midbrain in OSA in this exploratory study. We used a recently developed accelerated 2D magnetic resonance spectroscopy (2D-MRS) technique, compressed sensing-based 4D echo-planar J-resolved spectroscopic imaging (4D-EP-JRESI), to measure metabolites in the midbrain of 14 OSA (mean age ± SD:54.6 ± 10.6 years; AHI:35.0 ± 19.4; SAO_2 min:83 ± 7%) and 26 healthy control (50.7 ± 8.5 years) subjects. High-resolution T1-weighted scans allowed voxel localization. MRS data were processed with custom MATLAB-based software, and metabolite ratios calculated with respect to the creatine peak using a prior knowledge fitting (ProFit) algorithm. The midbrain in OSA showed decreased *N*-acetylaspartate (NAA; OSA:1.24 ± 0.43, Control:1.47 ± 0.41; $p = 0.03$; independent samples *t*-test), a marker of neuronal viability. Increased levels in OSA over control subjects appeared in glutamate (Glu; OSA:1.23 ± 0.57, Control:0.98 ± 0.33; $p = 0.03$), ascorbate (Asc; OSA:0.56 ± 0.28, Control:0.42 ± 0.20; (50.7 ± 8.5 years; $p = 0.03$), and myo-inositol (ml; OSA:0.96 ± 0.48, Control:0.72 ± 0.35; $p = 0.03$). No differences between groups appeared in γ-aminobutyric acid (GABA) or taurine. The midbrain in OSA patients shows decreased NAA, indicating neuronal injury or dysfunction. Higher Glu levels may reflect excitotoxic processes and astrocyte activation, and higher ml is also consistent with glial activation. Higher Asc levels may result from oxidative stress induced by intermittent hypoxia in OSA. Additionally, Asc and Glu are involved with glutamatergic processes, which are likely upregulated in the midbrain nuclei of OSA patients. The altered metabolite levels help explain dysfunction and structural deficits in the midbrain of OSA patients. © 2017 IBRO. Published by Elsevier Ltd. All rights reserved.

Neurochemical abbreviations with conventional capitalization: Asc, ascorbate; Asp, aspartate; Ch, choline; GABA, gamma-aminobutyric acid; Gln, glutamine; Glu, glutamate; Gly, glycine; GPC, glycerophosphorylcholine; GSH, glutathione; ml, myo-inositol; NAA, *N*-acetylaspartate; NAAG, *N*-acetylaspartate glutamate; PCh, phosphocholine; PE, phosphoethanolamine; Scy, scyllo-inositol; Tau, taurine; Thr, threonine.

Key words: intermittent hypoxia, autonomic, sleep-disordered breathing, periaqueductal gray, respiration, magnetic resonance spectroscopy.

INTRODUCTION

The defining feature of obstructive sleep apnea (OSA) is the occurrence of repeated airway collapses leading to successive cessation and restoration of airflow during sleep, with resultant exposure of the brain to intermittent hypoxia, excessive CO_2 levels, and repeated, large swings in blood pressure. Such exposures lead to overall and regional sites of brain injury, which presumably are responsible for multiple deficits in cardiovascular, hormonal, cognitive, and memory functions in the syndrome (Berry et al., 2012; Hudgel et al., 2012; Franklin and Lindberg, 2015). The processes underlying failure of the upper airway musculature during sleep with continued diaphragmatic efforts remain unclear, but several of the necessary sensory and motor control elements required for eupneic breathing lie within the midbrain; sites within the midbrain show injury or impaired responses to challenges in OSA (Harper et al., 2003; Macey et al., 2003, 2006, 2008).

The damaged midbrain sites are unlikely to be solely responsible for the wide range of neural influences that

*Correspondence to: P. M. Macey, UCLA School of Nursing, 700 Tiverton Avenue, Los Angeles, CA 90095-1702, United States.
E-mail address: pmacey@ucla.edu (P. M. Macey).
Abbreviations: 4D-EP-JRESI, accelerated 4D echo-planar J-resolved spectroscopic imaging; AHI, apnea–hypopnea index; BOLD, blood oxygen level dependent; CPAP, continuous positive airflow pressure; MRI, magnetic resonance imaging; MRS, magnetic resonance spectroscopy; MSNA, muscle sympathetic nerve activity; NUS, non-uniform undersampling; OSA, obstructive sleep apnea; TE, echo time; TR, repetition time; VOI, volume of interest.

contribute to the physiological deficits emerging in OSA. The midbrain is the recipient of projections from more-rostral and more-caudal sites that are also damaged in the syndrome, and serve essential timing and modulating influences on those descending and ascending projections. Among the damaged rostral sites projecting to the midbrain, the insular and ventromedial frontal cortices (Macey et al., 2008; Yaouhi et al., 2009; Joo et al., 2013; Kumar et al., 2014; Tummala et al., 2016) exert influences on cardiovascular and breathing systems; the midbrain contains many nuclei with major cardiovascular and breathing modulation and timing roles. While the final common pathways for outflow to upper airway and diaphragmatic respiratory musculature and for sympathetic and parasympathetic outflow to the cardiovascular system lie within the medulla, many modulatory systems, including those of the midbrain, affect those outflows (Davis et al., 1996; Subramanian, 2013). Principal drives to both the diaphragm and the upper airway muscles are CO_2 and O_2, followed by transient changes in blood pressure (Trelease et al., 1985). Sites within the midbrain play significant roles to all three drives (Harper et al., 1998, 2000, 2005; Woo et al., 2005). People with a lack of CO_2 sensitivity, such as those with congenital central hypoventilation syndrome, show impaired functional MRI signals in portions of the midbrain to hypercarbia, hypoxia (Macey et al., 2005), and forced expiration (Macey et al., 2004, 2005). The midbrain periaqueductal gray (PAG) projects to medullary cardiovascular and respiratory areas, and includes lateral and dorsomedial subregions involved in respiratory musculature control (Faull et al., 2015). Neurons in the PAG are synchronized with breathing cycles during sleep (Ni et al., 1990), and the structure is involved with modulation of respiratory rhythm and activity (Dampney et al., 2013; Farmer et al., 2014; Subramanian and Holstege, 2014). In animal models, the midbrain red nuclei are involved in coordinating responses to hypoxia (Waites et al., 1996; Ackland et al., 1997), a significant issue in a condition associated with repeated, extreme hypoxia exposure (Berry et al., 2012), and is presumably mediated through projections to the cerebellum (Granziera et al., 2009); the cerebellum is also damaged in OSA (Macey et al., 2008), leaving potential for impaired coordination.

The evidence that midbrain structural and functional alterations in OSA contribute to pathophysiology and symptoms of the disorder is substantial, considering the injury sites and nature of challenges that elicited the functional outcomes. Functional MRI studies show increased activation of the ventral and dorsal midbrain during inspiratory loading exercises (Macey et al., 2006, 2003) and decreased activity during cold pressor and expiratory loading challenges in OSA (Harper et al., 2003; Macey et al., 2003). Elevated muscle sympathetic nerve activity (MSNA) correlates with altered Blood Oxygen-Level-Dependent (BOLD) signals in the midbrain in OSA, suggesting a midbrain role in eliciting the high sympathetic tone in the sleep disorder (Fatouleh et al., 2014; Lundblad et al., 2014). CBF is decreased in the right midbrain of OSA subjects (Yadav et al., 2013), which

may reflect lower perfusion demand, perhaps from an altered functional state (for example, lower tonic activity), or impaired cerebral perfusion. Structural changes consistent with inflammatory or glial changes, namely diffusion decreases and volume increases, appear in the hypothalamus in OSA (Lundblad et al., 2014; Tummala et al., 2016), which projects heavily to the midbrain (Sakuma and Tada, 1984; Thompson and Swanson, 1998). The combined data suggest that the midbrain is compromised in OSA, potentially interfering with regulatory roles for cardiovascular and breathing control, as well as other physiological functions in the disorder. Although the MRI findings cannot further distinguish the nature of pathologies, we can gain understanding of what processes might lead to injury and dysfunction by examining chemicals, such as markers of cellular integrity, neuronal concentration, oxidative stress, and neurotransmitter levels.

Magnetic resonance spectroscopy (MRS) allows examination of differences in OSA in relatively abundant metabolites. Previous OSA spectroscopy studies found differences in neurochemical levels, such as decreased N-acetylaspartate (NAA), a neuronal marker, and increased levels of the excitatory neurotransmitter glutamate, in limbic brain regions including the hippocampus, thalamus, and putamen (Sarma et al., 2014, 2016). These findings suggest neural injury and increased excitation. Using "2-dimensional" spectroscopy, we showed the insulae have altered neurotransmitter levels bilaterally, including low GABA and high glutamate in OSA (Macey et al., 2016). These large differences in neurochemical levels likely affect the function of the structure, presumably leading to a more excitatory state (lower inhibition from lower GABA, higher excitation from higher glutamate). The insulae, key autonomic regulatory regions, project to the hypothalamus and midbrain nuclei to help regulate sympathetic outflow (Otake et al., 1994; Kurth et al., 2010); altered midbrain neurochemical levels would compromise that sympathetic regulation, as well as other functional processes. The intermittent hypoxia of OSA leads to widespread excitotoxic processes, which should be accompanied by high levels of glutamate.

The objective was to assess multiple midbrain metabolite alterations in OSA subjects using 2D MRS spectroscopy, and to interpret how such changes might contribute to the structural and functional alterations, and to the symptoms of autonomic dysfunction. The evaluation required new procedures for evaluating neurotransmitter levels, with a short scan time for often-ill patients, while still collecting spectral characteristics of multiple neurotransmitters. Assessment of NAA, glutamate, GABA, and other neurochemicals related to oxidative stress can help understand dysfunction and possible neurodegenerative processes that may be present in OSA. Measurements of levels of neurotransmitters contributing to function in the midbrain (see Kazemi, 2006 for review) could help determine processes mediating the previously found structural injury, assisting in understanding of mechanisms of dysfunction in OSA.

Experimental procedures

We studied 14 OSA patients (mean age = 54.6 ± 10.6 years; 9 male; mean AHI:35.0 ± 19.4 events/ hour; SAO_2 min:83 ± 9%) and 26 healthy subjects (mean age = 50.7 ± 8.5 years; 11 male). Participant characteristics are shown in Table 1. We missed collecting BMI on some control participants, so those data are incomplete. Patients were diagnosed at the UCLA Sleep Disorders Center. No participants had a history of head trauma or disease, current depressive or anxiety mental illness, cancer, epilepsy or major cardiac disease (infarct, stroke, bypass surgery). Any history of a psychotic mental illness, substance, or bipolar depressive disorder was exclusionary. No participants had other pulmonary disease or diagnosed sleep disorder. OSA patients were not assessed for sustained nocturnal hypoxia or daytime hypoxia. Alcohol consumption was not assessed. Current usage of medication in the following categories was exclusionary: psychotropic (anti-depressant, anti-anxiety, antipsychotic) beta-blockers, ACE inhibitors and anti-epileptic. We did not assess use of sleep aids. No participants were engaged in shift work or had recently traveled from a different time zone (within the week prior to scanning). Patients were never treated for sleep disordered breathing apart from two with a prior history of CPAP use. Healthy subjects were screened via interview to exclude OSA as well as other sleep disorders. Procedures were approved by the UCLA Institutional Review Board, and participants provided written, informed consent.

Participants were mostly scanned during weekend days anytime between 8 AM and 6 PM. Participants were instructed to refrain from caffeine and alcohol for 24 h prior to their visit. Metabolites were measured with a novel 2D-magnetic resonance spectroscopy (MRS) method, accelerated 4D echo-planar J-resolved spectroscopic imaging (4D-EP-JRESI) (Sarma et al., 2014). The procedure uses non-uniform undersampling (NUS) for acceleration with compressed sensing reconstruction. Data were collected on a 3T Trio-Tim MRI scanner (Siemens Medical Solutions, Erlangen, Germany) using an 8-channel phased-array head coil. High-resolution T_1-weighted scans in the sagittal plane were acquired for voxel localization prior to the spectroscopic scans. NUS-based 4D-EP-JRESI was performed over a coronal slice covering bilateral regions encompassing left

and right areas of the midbrain using the parameters: TR/ TE = 1.5 s/30 ms, field-of-view = 24×24 cm^2 with 16×16 grids, voxel resolution = $1.5 \times 1.5 \times 1.5$ cm^3, 512 bipolar echo pair, 64 Δt_1 increments (1 ms), averages = 2, and $4\times$ acceleration. An example of a midbrain volume-of-interest (VOI) for one OSA subject is shown in Fig. 1. The VOI extends across most of the midbrain, but excludes the most lateral and anterior/posterior regions.

The MRS data were extracted and post-processed using a custom MATLAB-based library of programs (The Mathworks, Natick, MA, USA). Data post-processing involved raw data reconstruction, and a series of steps described elsewhere (Sarma et al., 2016, 2014). Metabolite ratios with respect to creatine were calculated using the prior knowledge fitting (ProFit) algorithm with Cramer Lower Bounds (Schulte and Boesiger, 2006; Fuchs et al., 2014), optimized for processing the Siemens data. Quality checking was performed on the spectra by visual inspection, and fit criteria for ProFit consisted of Cramer-Rao Lower Bound < 20%. Other criteria for rejection of spectra were based on patient movement or poor water suppression. Our approach results in satisfactory reliability for more abundant chemicals, with coefficients of variation (CV) ranging from < 10% to 30%. In unpublished repeatability data from our earlier insula study (Macey et al., 2016), we performed three scans on three subjects and found CVs for Glu and GABA ranging from 0.3% to 30%. Of note, for Glu and GABA in 2/3 subjects, the right showed lower CVs than the left.

Statistical analyses were performed with MATLAB software (version 9.1). Chemical levels were compared between OSA and control subjects with independent sample t-tests (MATLAB ttest2 function). Independent samples t-tests allow for different variability in each group. Relationships between metabolites were assessed within and between groups using pairwise correlation (MATLAB corrcoeff function). Specifically, the correlation between metabolites was calculated and assessed for significance in OSA and control groups, and additionally the relationships were tested for significant differences between these groups (all tests performed with MATLAB corrcoeff). Based on our earlier findings (Macey et al., 2016; Sarma et al., 2016, 2014; Yadav et al., 2014), we tested a priori hypotheses that Cho, GABA, Glu, mI, NAA, PE, PCh and Scy would show group differences. Two other chemicals strongly associated with oxidative stress, and hence we predict OSA,

Table 1. Characteristics of OSA and control subjects, with separation by sex. Note that BMI was missing for some control subjects

	Mixed		Female		Male	
	OSA $N = 14$ Mean ± std	CONTROL $N = 26$ Mean ± std	OSA $N = 5$ Mean ± std	CONTROL $N = 12$ Mean ± std	OSA $N = 9$ Mean ± std	CONTROL $N = 14$ Mean ± std
Age (years)	47.2 ± 10.5	50.1 ± 8.5	51.0 ± 7.4	51.3 ± 7.1	45.0 ± 11.6	50.1 ± 9.9
BMI (m^2/kg)	30.3 ± 4.3	27.2 ± 6 ($N = 15$)	32.5 ± 6.5	26.0 ± 6.3 ($N = 6$)	29.0 ± 1.7	28.0 ± 7.0 ($N = 8$)
Sleep parameters						
AHI (events/hour)	29.8 ± 14.8		27.6 ± 20.4		31.2 ± 11.4	
SaO$_2$ (minimum%)	82.5 ± 8.9		88.5 ± 4.8		79.5 ± 9.1	
SaO$_2$ (baseline%)	94.1 ± 2.8		94.6 ± 2.3		93.8 ± 3.1	

Midbrain voxel location in coronal, axial and sagittal views (15 mm³ left/right)
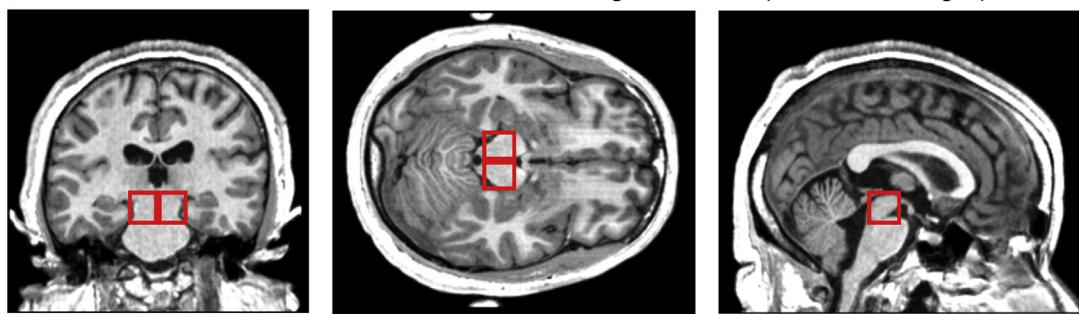
Fig. 1. Location of midbrain VOI for one male OSA subject. Red outline (15 mm³) is displayed on subject's anatomical scan. (For interpretation of the references to color in this figure legend, the reader is referred to the web version of this article.)

are Asc and lactate; however, the latter is only detected at high concentrations (Govindaraju et al., 2000). Correction for multiple comparisons was applied to the remaining metabolites using the Bonferroni method. For significant findings, we ran additional correlations of metabolite levels with and BMI and sleep parameters for the OSA group.

RESULTS

Concentrations of 17 metabolites in 26 healthy and 14 OSA subjects (Table 2, example spectra in Fig. 2, group results Fig. 3) were evaluated. Some data were excluded due to inadequate quality spectra, as determined either by initial visual inspection or by failure to meet quality control criteria. Lactate is one chemical that can be measured at higher concentrations, but was not observed, likely due to low concentrations. Success rates were similar for OSA and control groups.

Differences between OSA and control subjects emerged in NAA, glutamate, ascorbate, and myo-inositol (Fig. 3). The OSA group showed lower NAA, and higher glutamate, ascorbate and myo-inositol. No differences emerged in GABA, choline, or other metabolites. The findings were not altered by correction for multiple comparisons across Asp, GPC, Gln, Gly, GSH, NAAG, Tau, and Thr. If the measurements had been considered independent with a priori hypothesis of OSA-control differences, the multiple comparisons correction across the 17 chemicals would have resulted in no significant findings.

In controls, ascorbate exhibited significant positive correlations with four metabolites (Glu, GSH, PE, Thr), glutamate with three (Asc, Ch, GSH), and myo-inositol with four (Gly, GSH, PE, Tau), while NAA showed a significant negative correlation with three metabolites (GSH, NAAG, Thr; Table 3 and Fig. 4). Glutamate and ascorbate had significant positive correlations; however, there was no significant relationship between these two chemicals and myo-inositol and NAA. In OSA subjects, ascorbate had positive correlations with four metabolites (Asp, Glu, GSH, Thr), glutamate with four (Asc, Asp, GSH, PE), myo-inositol with three (GABA, Gly, Thr), and NAA with five (GPC, GSH, PCh, Scy, Thr; Table 3,

Table 2. Metabolite levels in subsets of 14 OSA and 26 control combined female and male subjects (P: independent samples t-test for group differences). SD = standard deviation, CV = coefficient of variation, N = number of subjects with valid measures. Order is by convention, based on concentration and location along spectrum. * and bold indicates $P < 0.05$.

Chemical		CV	OSA			Control			P uncorrected (OSA vs Control)
			Mean	SD	N	Mean	SD	N	
NAA	*N-acetylaspartate*	31	**1.24**	± 0.43	*14*	**1.47**	± 0.41	*26*	***0.027**
PCh	*phosphocholine*	84	0.07	± 0.05	*4*	0.08	± 0.07	*11*	0.602
GPC	*glycerophosphorylcholine*	54	0.19	± 0.11	*14*	0.22	± 0.11	*26*	0.162
Ch	*choline*	69	0.18	± 0.09	*9*	0.13	± 0.11	*20*	0.087
Asp	*aspartate*	54	0.58	± 0.33	*13*	0.49	± 0.24	*20*	0.253
GABA	*gamma-aminobutyric acid*	52	0.32	± 0.21	*8*	0.30	± 0.11	*14*	0.702
Gln	*glutamine*	43	0.45	± 0.18	*13*	0.39	± 0.17	*23*	0.135
Glu	*glutamate*	42	**1.23**	± 0.57	*14*	**0.98**	± 0.33	*26*	***0.030**
Gly	*glycine*	56	0.14	± 0.09	*9*	0.13	± 0.07	*22*	0.532
Asc	*ascorbate*	52	**0.56**	± 0.28	*13*	**0.42**	± 0.20	*25*	***0.026**
GSH	*glutathione*	52	0.30	± 0.13	*11*	0.28	± 0.16	*24*	0.584
ml	*myo-inositol*	51	**0.96**	± 0.48	*12*	**0.72**	± 0.35	*22*	***0.047**
NAAG	*N-acetylaspartylglutamate*	81	0.38	± 0.28	*14*	0.37	± 0.31	*24*	0.889
PE	*phosphoethanolamine*	45	0.70	± 0.31	*13*	0.58	± 0.27	*20*	0.149
Tau	*taurine*	97	0.39	± 0.49	*6*	0.35	± 0.27	*15*	0.778
Scy	*scyllo-inositol*	52	0.07	± 0.04	*12*	0.06	± 0.03	*25*	0.390
Thr	*threonine*	50	0.69	± 0.34	*13*	0.55	± 0.26	*25*	0.067

A. OSA

B. CONTROL

C. BASIS SET
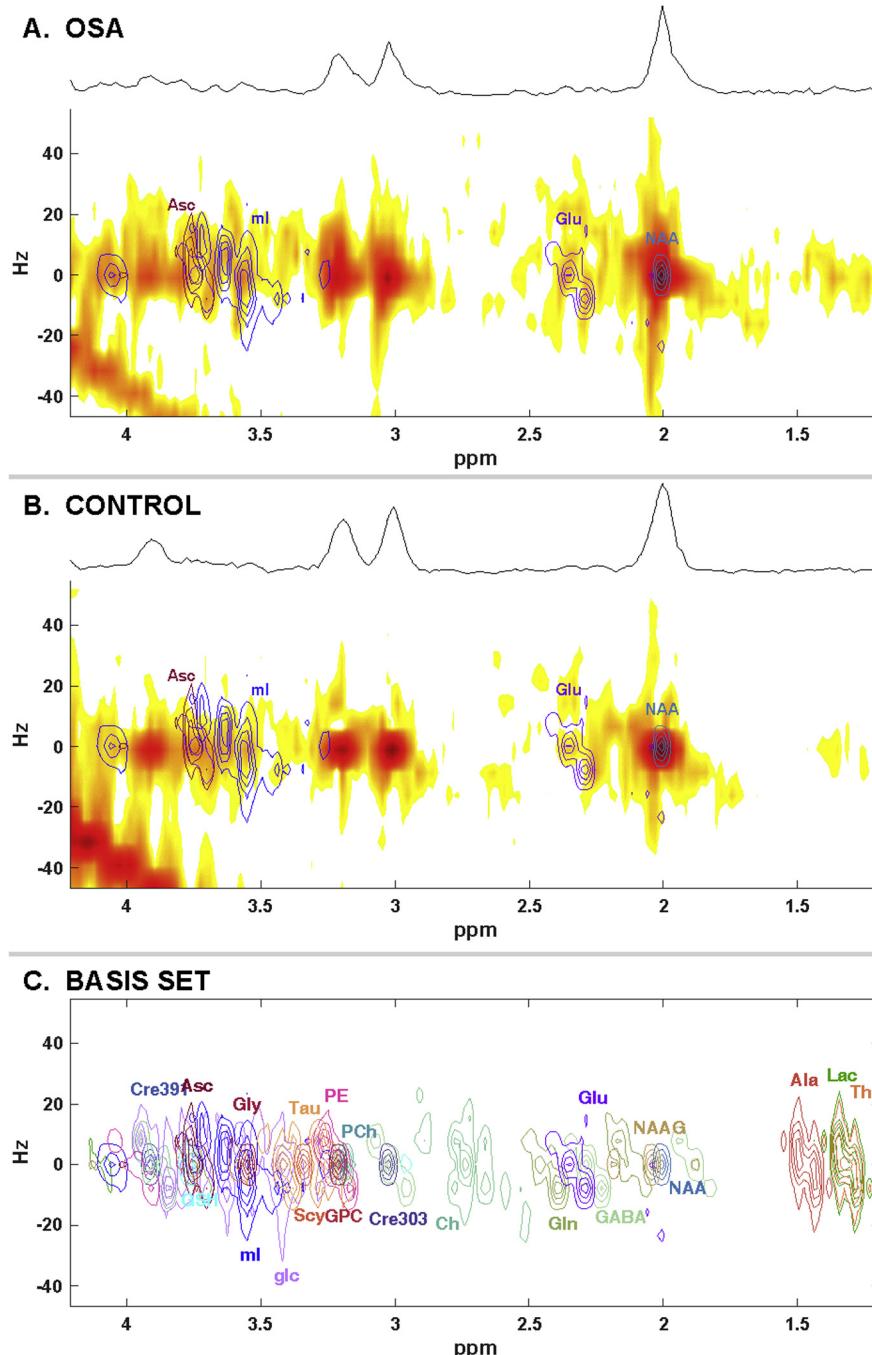
Fig. 2. Example 2D-MRS spectra from the midbrain in (A) OSA (56 year female) and (B) control (53-year-old male) subjects, with resonances of chemicals with significant group differences indicated (Glu = glutamate, Asc = ascorbate, mI = myo-inositol, NAA = N-acetylaspartate, Tau = taurine; other chemicals listed in Table 2). (C) Basis set for all chemicals detected, reflecting resonances in 2D spectral space (key in Table 2; additional chemicals: Ala = alanine, Cre391/Cre303 = creatine, Lacx = lactate). In A and B, 1D spectra at f = 0 Hz line are plotted above the 2D display; the NAA peak is visible at ~2 ppm.

Fig. 4). Significant group differences in correlations between OSA and control groups appeared in the following chemical pairs: glutamate–aspartate, GABA–NAAG, glycine–taurine, NAA–phosphocholine, NAAG–scyllo-inositol, and threonine–glycerophosphorylcholine. In the OSA group, the Glu, NAA, Asc and mI levels

were not correlated with BMI, AHI, SaO$_2$ nadir, or SaO$_2$ baseline (Fig. 5).

DISCUSSION

Four of 17 neurochemicals in the midbrain of OSA subjects showed altered levels, compared to controls. The nature of the alterations suggests that the midbrain in OSA is associated with lower neuronal density, higher glial concentration, and the presence of oxidative stress and excitotoxicity. While these phenomena are not unexpected, the findings provide direct, in vivo chemical evidence of such processes. The pattern of alterations differs from the insula, hippocampus and thalamus (Sarma et al., 2016, 2014; Yadav et al., 2014), suggesting midbrain-specific pathology accompanying OSA.

The low NAA in OSA subjects found in the midbrain is consistent with similar observations in other brain areas. Decreased NAA has been shown earlier in the hippocampus, insula, thalamus and putamen, as well as in occipital, temporal, and frontal regions (Sarchielli et al., 2008; Algin et al., 2012; O'Donoghue et al., 2012; Kizilgoz et al., 2013; Sarma et al., 2016, 2014; Tonon et al., 2007; Yadav et al., 2014). One study showed increased NAA in the left hippocampus as a ratio of creatine (Bartlett et al., 2004), but changes were attributed to lower creatine, as opposed to higher NAA; furthermore, the sample was small (8 OSA vs. 5 control). In the brain, NAA is present only in neurons, and can be a neuronal marker (Simmons et al., 1991), reflecting mitochondrial function in neurons (Moffett et al., 2007). Changes in NAA can therefore reflect both neuron loss and altered function (Demougeot et al., 2001). Changes in NAA concentrations occur with neuronal injury in neurodegenerative disease (Schuff et al., 2006), and the decreased levels of NAA in the midbrain and hypothalamus found here are consistent with fewer neurons in these brain regions in OSA. The alternative interpretation of lower NAA would be reduced activation of midbrain neurons in OSA; such a phenomenon may be present, but we have little prior evidence to support or refute such a possibility. Given the combined findings of lower NAA in
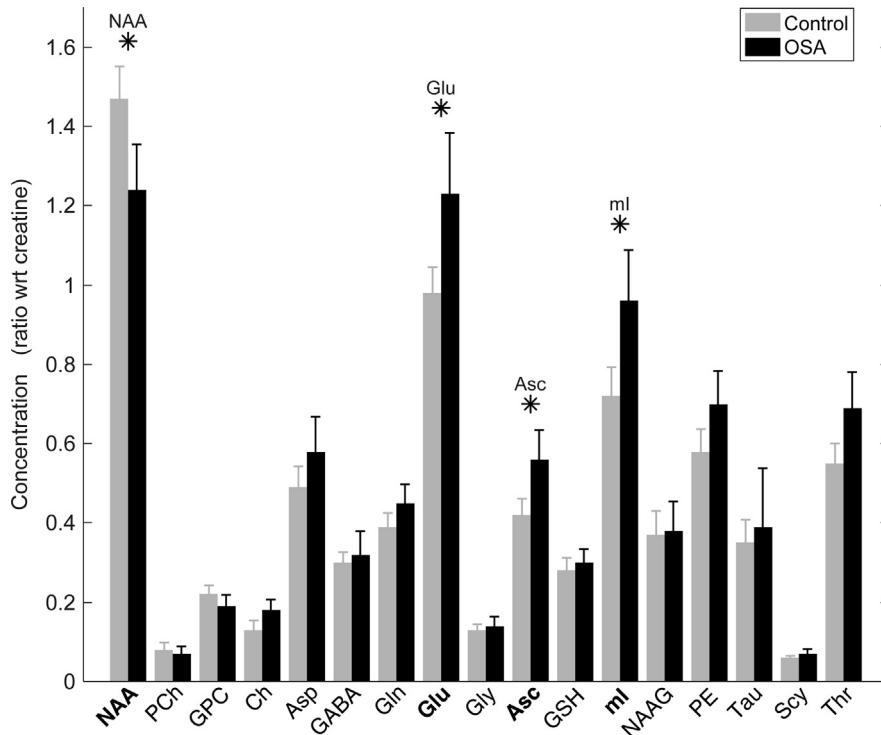
Fig. 3. Midbrain chemical levels in 14 OSA and 26 healthy control subjects (mean ± SEM); see Table 2. Significant group differences indicated by "*" and bold label. Key in Table 2.

multiple regions, neurodegenerative processes or other modes of neuronal death are likely present in widespread brain areas in OSA.

Glutamate was elevated in the midbrain of OSA subjects. As with decreased NAA, the present findings are consistent with earlier studies that showed increased glutamate in other limbic regions as well as the temporal and frontal brain regions of OSA (Yadav et al., 2014; Sarma et al., 2016). Glutamate is the most common excitatory metabolite in the brain (Meldrum, 2000); thus, high levels of glutamate in OSA are likely associated with a more active state in the midbrain region. Given the lower NAA, the higher glutamate levels could reflect greater astrocyte activation (Kimelberg et al., 1990; Szatkowski et al., 1990), perhaps as a compensatory mechanism attempting to correct for lower neural activity. In addition to altering function, high levels of extracellular glutamate lead to excitotoxicity and in apoptosis of neurons (Fung et al., 2007). Hence, high glutamate is consistent with low NAA if the latter is considered a marker of neuronal cells (as opposed to neuronal function). Increased glutamate under hypoxic conditions results from the mismatch of the rates of glycolysis and oxidative metabolism in the brain, which lead to an eventual shift in the aspartate aminotransferase reaction to aspartate consumption and glutamate formation (Siesjo et al., 1976; Siesjo, 1978; Erecinska and Silver, 1990; Stagg and Rothman, 2014). Since glutamate is high across multiple regions (Macey et al., 2016; Sarma et al., 2016, 2014), the high glutamate may reflect widespread pathological processes in OSA.

Myo-inositol levels were high in the midbrain in OSA. Myo-inositol is most commonly found in brain glial cells, and is considered a marker of astroglia and microglia activation (Chang et al., 1998; Bitsch et al., 1999). The chemical is involved in clearance of byproducts of cell-damaging processes (Gehrmann et al., 1995). Therefore, high levels of mI in OSA could reflect astrocyte activation, possibly to intermittent hypoxia, which in animal models results in up to a ten-fold increase in glial cell size (Aviles-Reyes et al., 2010); astrocyte swelling is one mechanism that can lead to glutamate release (Kimelberg et al., 1990). Increased mI in OSA was similarly reported in limbic regions of the insular cortex, thalamus, putamen and the temporal and frontal brain regions in earlier spectroscopy studies (Sarma et al., 2016, 2014; Yadav et al., 2014). Increased limbic levels of mI accompany dementia and mild cognitive impairment (Shinno et al., 2007; Ohnishi et al., 2013), suggesting a possible link with memory deficits in OSA (Wallace and Bucks, 2013). The combined findings of high myo-inositol in multiple brain regions of OSA indicate microglial activation is likely a global, rather than region-specific phenomenon in the sleep disorder.

In OSA, intermittent hypoxia leads to oxidative stress (Xu et al., 2004), which in turn leads to excess of free radicals including ascorbate (Grebe et al., 2006), which we found elevated here. Ascorbate is an antioxidant involved in the glutamate reuptake process (Rebec and Pierce, 1994). The significant positive correlation with glutamate in both OSA and control groups likely reflects this relationship. Ascorbate is a marker of oxidative stress in its free radical form (Buettner and Jurkiewicz, 1993), and the high levels provide evidence that this process occurs in the midbrain of OSA subjects. Ascorbate also aids the reuptake of glutamate, but the increased Asc is not sufficient to keep or return glutamate to normal levels in the present findings.

Structural changes in brain tissue may be, in part, reflected in the chemical changes seen in the midbrain, especially lower NAA and higher mI. People with OSA show altered organization of axonal tracts, reflected as higher diffusion kurtosis (Tummala et al., 2016). This measure is sensitive to various structural patterns, but in the context of the sleep disorder, the increase in kurtosis likely reflects less coherent axonal tracts, i.e., either smaller or more damaged tracts combined, or more crossing fibers in a region compared with healthy people (Jensen et al., 2005). Volume increases appear in the ventral midbrain in OSA, which would be adjacent to, or only slightly overlapping the measurements in the present

Table 3. (A) Correlation table for first 9/17 chemicals, separated by group. Correlation coefficients are shown (OSA = "R OSA" and Control = "R Con"). Significant (*p* < 0.05) within-group correlations are indicated by (*). *P*-values for between-group differences in correlations are shown, with *p* < 0.05 highlighted in bold and "*". Scatterplots are shown in Fig. 4. (B) Correlation table for last 8/17 chemicals, separated by group. Correlation coefficients are shown (OSA = "R OSA" and Control = "R Con"). Significant (p < 0.05) within-group correlations are indicated by (*). P-values for between-group differences in correlations are shown, with p < 0.05 highlighted in bold and "*". Scatterplots are shown in Fig. 4.

(A)

	Asc R Con	Asc R OSA	Asc p	Asp R Con	Asp R OSA	Asp p	Ch R Con	Ch R OSA	Ch p	GABA R Con	GABA R OSA	GABA p	Gln R Con	Gln R OSA	Gln p	Glu R Con	Glu R OSA	Glu p	Gly R Con	Gly R OSA	Gly p	GPC R Con	GPC R OSA	GPC p	GSH R Con	GSH R OSA	GSH p
Asc				0.152	0.611 (*)	0.128	0.369	0.596	0.415	0.349	−0.213	0.113	−0.031	0.134	0.649	0.525 (*)	0.638 (*)	0.638	0.174	0.522	0.272	0.274	−0.389	0.059	0.765 (*)	0.938 (*)	0.051
Asp	0.152	0.611 (*)	0.128				0.118	0.394	0.417	0.491	−0.099	0.082	0.462 (*)	0.470	0.978	0.058	0.885 (*)	*0.000	−0.054	−0.102	0.895	−0.053	−0.123	0.847	0.420	0.659 (*)	0.349
Ch	0.369	0.596	0.415	0.118	0.394	0.417				0.431	0.220	0.517	−0.049	0.261	0.389	0.561 (*)	0.528	0.897	0.238	0.129	0.758	−0.433 (*)	−0.325	0.729	0.618 (*)	0.693 (*)	0.720
GABA	0.349	−0.213	0.113	0.491	−0.099	0.082	0.431	0.220	0.517				−0.009	0.251	0.470	0.358	−0.004	0.302	0.251	0.194	0.870	−0.249	−0.481	0.461	0.351	−0.164	0.147
Gln	−0.031	0.134	0.649	0.462 (*)	0.470	0.978	−0.049	0.261	0.389	−0.009	0.251	0.470				−0.092	0.385	0.175	−0.274	−0.116	0.653	0.009	−0.024	0.928	−0.146	0.053	0.585
Glu	0.525 (*)	0.638 (*)	0.638	0.058	0.885 (*)	*0.000	0.561 (*)	0.528	0.897	0.358	−0.004	0.302	−0.092	0.385	0.175				0.024	0.093	0.849	0.384	−0.249	0.072	0.461 (*)	0.627 (*)	0.516
Gly	0.174	0.522	0.272	−0.054	−0.102	0.895	0.238	0.129	0.758	0.251	0.194	0.870	−0.274	−0.116	0.653	0.024	0.093	0.849				−0.226	−0.588 (*)	0.226	0.478 (*)	0.438	0.889
GPC	0.274	−0.389	0.059	−0.053	−0.123	0.847	−0.433 (*)	−0.325	0.729	−0.249	−0.481	0.461	0.009	−0.024	0.928	0.384	−0.249	0.072	−0.226	−0.588 (*)	0.226				−0.114	−0.478	0.268
GSH	0.765 (*)	0.938 (*)	0.051	0.420	0.659 (*)	0.349	0.618 (*)	0.693 (*)	0.720	0.351	−0.164	0.147	−0.146	0.053	0.585	0.461 (*)	0.627 (*)	0.516	0.478 (*)	0.438	0.889	−0.114	−0.478	0.268			
ml	0.275	0.268	0.984	0.251	−0.119	0.305	0.422	0.242	0.578	0.434	0.625 (*)	0.464	−0.390	0.147	0.127	0.168	0.074	0.794	0.416 (*)	0.582 (*)	0.543	−0.089	−0.449	0.282	0.449 (*)	0.196	0.438
NAA	−0.118	−0.384	0.436	−0.337	−0.354	0.959	−0.217	−0.160	0.873	0.202	−0.019	0.542	0.104	0.214	0.757	−0.064	−0.292	0.519	−0.331	−0.065	0.448	0.282	0.575 (*)	0.319	−0.498 (*)	−0.641 (*)	0.560
NAAG	−0.136	0.008	0.694	0.289	0.186	0.765	0.143	0.578	0.160	−0.011	0.642 (*)	*0.035	−0.063	0.203	0.463	0.150	0.350	0.558	−0.200	−0.149	0.885	−0.211	−0.321	0.746	0.228	0.206	0.950
PCh	−0.258	−0.217	0.905	−0.243	−0.264	0.952	−0.628 (*)	−0.499	0.603	0.087	−0.315	0.260	−0.200	−0.668	0.099	−0.386	0.012	0.253	−0.297	0.257	0.121	−0.133	−0.359	0.509	−0.305	−0.059	0.485
PE	0.488 (*)	0.468	0.944	0.508 (*)	0.421	0.762	0.181	0.325	0.673	0.545 (*)	0.172	0.233	−0.174	0.175	0.336	0.401	0.673 (*)	0.286	0.409	0.255	0.635	0.242	−0.370	0.083	0.579 (*)	0.369	0.456
Scy	0.330	0.336	0.985	0.099	0.406	0.366	0.368	0.564	0.491	0.499 (*)	0.309	0.533	0.100	0.122	0.952	0.123	0.439	0.343	0.304	−0.036	0.339	−0.198	−0.340	0.675	0.354	0.539	0.524
Tau	0.218	0.404	0.571	0.219	0.296	0.822	0.672 (*)	0.831 (*)	0.302	0.302	0.123	0.609	−0.065	0.124	0.606	0.279	0.550	0.365	0.664 (*)	0.016	*0.033	−0.445 (*)	−0.325	0.699	0.545 (*)	0.431	0.684
Thr	0.455 (*)	0.687 (*)	0.339	0.134	0.449	0.341	0.172	0.493	0.319	−0.308	0.316	0.078	0.042	0.235	0.590	0.094	0.506	0.206	0.266	0.472	0.514	−0.140	−0.730 (*)	*0.032	0.413	0.789 (*)	0.086

(B)

|	ml R Con	ml R OSA	ml p	NAA R Con	NAA R OSA	NAA p	NAAG R Con	NAAG R OSA	NAAG p	PCh R Con	PCh R OSA	PCh p	PE R Con	PE R OSA	PE p	Scy R Con	Scy R OSA	Scy p	Tau R Con	Tau R OSA	Tau p	Thr R Con	Thr R OSA	Thr p
Asc	0.275	0.268	0.984	−0.118	−0.384	0.436	−0.136	0.008	0.694	−0.258	−0.217	0.905	0.488 (*)	0.468	0.944	0.330	0.336	0.985	0.218	0.404	0.571	0.455 (*)	0.687 (*)	0.339
Asp	0.251	−0.119	0.305	−0.337	−0.354	0.959	0.289	0.186	0.765	−0.243	−0.264	0.952	0.508 (*)	0.421	0.762	0.099	0.406	0.366	0.219	0.296	0.822	0.134	0.449	0.341
Ch	0.422	0.242	0.578	−0.217	−0.160	0.873	0.143	0.578	0.160	−0.628 (*)	−0.499	0.603	0.181	0.325	0.673	0.368	0.564	0.491	0.672 (*)	0.831 (*)	0.302	0.172	0.493	0.319
GABA	0.434	0.625 (*)	0.464	0.202	−0.019	0.542	−0.011	0.642 (*)	*0.035	0.087	−0.315	0.260	0.545 (*)	0.172	0.233	0.499 (*)	0.309	0.533	0.302	0.123	0.609	−0.308	0.316	0.078
Gln	−0.390	0.147	0.127	0.104	0.214	0.757	−0.063	0.203	0.463	−0.200	−0.668	0.099	−0.174	0.175	0.336	0.100	0.122	0.952	−0.065	0.124	0.606	0.042	0.235	0.590
Glu	0.168	0.074	0.794	−0.064	−0.292	0.519	0.150	0.350	0.558	−0.386	0.012	0.253	0.401	0.673 (*)	0.286	0.123	0.439	0.343	0.279	0.550	0.365	0.094	0.506	0.206
Gly	0.416 (*)	0.582 (*)	0.543	−0.331	−0.065	0.448	−0.200	−0.149	0.885	−0.297	0.257	0.121	0.409	0.255	0.635	0.304	−0.036	0.339	0.664 (*)	0.016	*0.033	0.266	0.472	0.514
GPC	−0.089	−0.449	0.282	0.282	0.575 (*)	0.319	−0.211	−0.321	0.746	−0.133	−0.359	0.509	0.242	−0.370	0.083	−0.198	−0.340	0.675	−0.445 (*)	−0.325	0.699	−0.140	−0.730 (*)	*0.032
GSH	0.449 (*)	0.196	0.438	−0.498 (*)	−0.641 (*)	0.560	0.228	0.206	0.950	−0.305	−0.059	0.485	0.579 (*)	0.369	0.456	0.354	0.539	0.524	0.545 (*)	0.431	0.684	0.413	0.789 (*)	0.086
ml				0.073	0.001	0.843	0.033	0.274	0.499	−0.248	−0.294	0.893	0.608 (*)	0.511	0.699	−0.102	0.260	0.314	0.620 (*)	0.280	0.232	0.007	0.594 (*)	0.065
NAA	0.073	0.001	0.843				−0.412 (*)	−0.410	0.994	0.065	−0.831 (*)	*0.001	0.003	−0.087	0.805	−0.209	−0.585 (*)	0.210	−0.264	−0.175	0.798	−0.499 (*)	−0.705 (*)	0.370
NAAG	0.033	0.274	0.499	−0.412 (*)	−0.410	0.994				0.300	0.062		−0.166	0.219		−0.051	0.788 (*)		−0.043	0.563		0.005	0.478	
PCh	−0.248	−0.294	0.893	0.065	−0.831 (*)	*0.001	0.300	0.062																
PE	0.608 (*)	0.511	0.699	0.003	−0.087	0.805	−0.166	0.219																
Scy	−0.102	0.260	0.314	−0.209	−0.585 (*)	0.210	−0.051	0.788 (*)																
Tau	0.620 (*)	0.280	0.232	−0.264	−0.175	0.798	−0.043	0.563																
Thr	0.007	0.594 (*)	0.065	−0.499 (*)	−0.705 (*)	0.370	0.005	0.478																
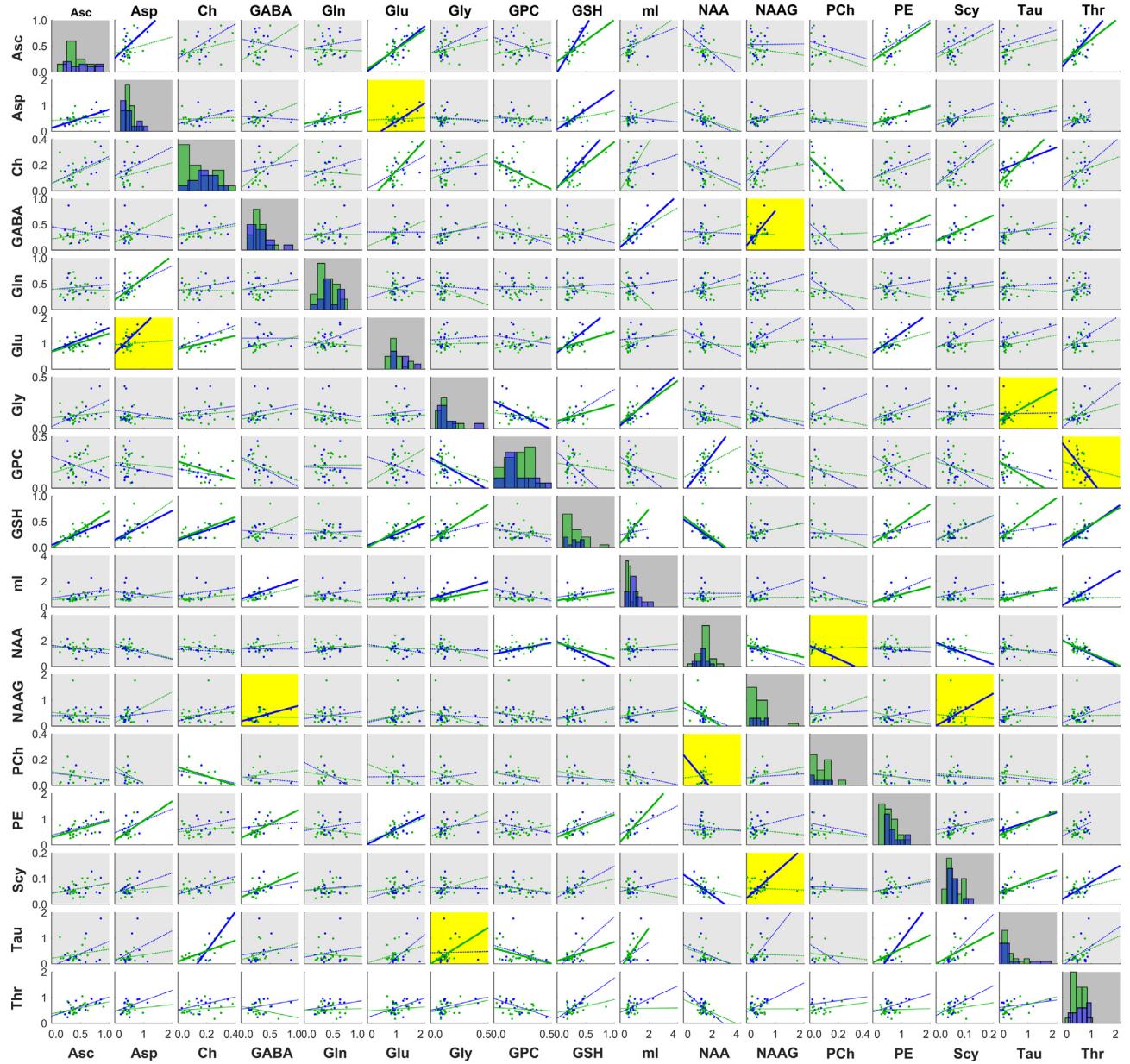
Fig. 4. Correlation plots of each combination of chemicals, and distributions, separated into OSA (blue) and control (green) groups. Center diagonal shows distributions. Other scatter plots show pairs of chemicals. Solid lines indicate a significant correlation. Plots with a yellow background indicate a significant group difference in correlations. Plots with a white background indicate one or both groups have a significant correlation. Plots with a gray background have no significant correlations. Key in Table 2. (For interpretation of the references to color in this figure legend, the reader is referred to the web version of this article.)

study (Lundblad et al., 2014). Such increases were reversed with continuous positive airway pressure treatment, suggesting a possible reduction of gliosis (Henderson et al., 2016). Evidence of such a mechanism could be provided in a future study by assessing whether a reduction in mI accompanies the reduction in volume. Oxidative stress also results in cell damage, and promotes inflammation (Haddad, 2002). Inflammation in the hypothalamus, specifically microglial activation, is associated with hypertension in rat models (Shi et al., 2010; Yoshimoto et al., 2010); the chemical changes in the present findings also suggest the presence of inflammation since Asc and markers of glial activation are increased.

The decreased levels of NAA suggest damage to neurons in OSA, consistent with reports of decreased gray matter and altered integrity of white matter tracts in OSA (Macey et al., 2002, 2008; Joo et al., 2010; Castronovo et al., 2014). However, not all those previously reported changes were localized in the midbrain.

Limitations include a lack of specificity about which midbrain structures were affected. The findings therefore represented neurochemical levels across a number of midbrain nuclei and different functional groups of neurons, and individual nuclei may have different concentration patterns than those found here. Methodological limitations include limited measurement
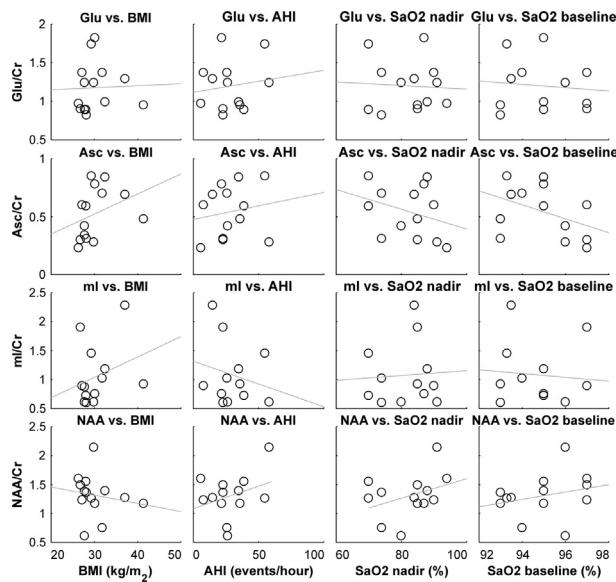
Fig. 5. Scatterplots of midbrain metabolite levels in 14 OSA subjects with respect to BMI and sleep parameters (AHI, SaO_2 nadir, and SaO_2 baseline). No correlations were significant.

reliability due to the sensitivity of the technique, and factors affecting reliability such as head motion and voxel selection. These factors are not group-specific, and should decrease sensitivity, so the most likely effect would be false negatives rather than false positives. Obesity, hypertension, diabetes (or pre-diabetes), depression and anxiety are factors strongly associated with OSA that each may influence the neural state. Thus, the degree to which OSA is independently linked to midbrain changes cannot be determined with the present findings. Time of day likely affects the midbrain state and hence metabolite levels; OSA patients frequently experience excessive tiredness in the morning, so presumably that group may show more time-of-day variability than the control group. However, there was no scan time systematic bias in either group, and the time of scanning varied from morning to early evening, so the effect would likely be one of increasing variability and therefore reducing sensitivity. Finally, the sample is relatively small, with further reductions in measures of specific metabolites following quality checking. The findings should therefore be viewed as exploratory. In a related caveat, the findings can only be considered statistically significant in the light of previous findings and animal models that support hypothesize OSA-related differences in metabolite levels. If the measures were considered without that context, no findings would survive correction for multiple comparisons. Finally, the 2D MRS approach is a large-area non-invasive measurement of neurochemicals in humans, and therefore does not replace but rather complements the precise identification available with animal models in terms of location, chemical type, and concentration levels.

In conclusion, the midbrain of individuals with OSA exhibits lower levels of NAA and higher levels of glutamate, mI and ascorbate than controls. The altered metabolite levels indicate neuronal loss and inflammation in these brain structures, both of which likely contribute to deficient physiological regulation including autonomic control such as increased sympathetic tone, hypertension and cardiovascular issues. Understanding the alterations in brain chemical levels will provide insights into processes of dysfunction in OSA and potential interventions to reduce the impact of injury to the affected areas.

REFERENCES

Ackland GL, Noble R, Hanson MA (1997) Red nucleus inhibits breathing during hypoxia in neonates. Respir Physiol 110:251–260.

Algin O, Gokalp G, Ocakoglu G, Ursavas A, Taskapilioglu O, Hakyemez B (2012) Neurochemical-structural changes evaluation of brain in patients with obstructive sleep apnea syndrome. Eur J Radiol 81:491–495.

Aviles-Reyes RX, Angelo MF, Villarreal A, Rios H, Lazarowski A, Ramos AJ (2010) Intermittent hypoxia during sleep induces reactive gliosis and limited neuronal death in rats: implications for sleep apnea. J Neurochem 112:854–869.

Bartlett DJ, Rae C, Thompson CH, Byth K, Joffe DA, Enright T, Grunstein RR (2004) Hippocampal area metabolites relate to severity and cognitive function in obstructive sleep apnea. Sleep Med 5:593–596.

Berry RB, Budhiraja R, Gottlieb DJ, Gozal D, Iber C, Kapur VK, Marcus CL, Mehra R, Parthasarathy S, Quan SF, Redline S, Strohl KP, Davidson Ward SL, Tangredi MM, American Academy of Sleep Medicine (2012) Rules for scoring respiratory events in sleep: update of the 2007 AASM Manual for the Scoring of Sleep and Associated Events. Deliberations of the Sleep Apnea Definitions Task Force of the American Academy of Sleep Medicine. J Clin Sleep Med 8:597–619.

Bitsch A, Bruhn H, Vougioukas V, Stringaris A, Lassmann H, Frahm J, Bruck W (1999) Inflammatory CNS demyelination: histopathologic correlation with in vivo quantitative proton MR spectroscopy. AJNR Am J Neuroradiol 20:1619–1627.

Buettner GR, Jurkiewicz BA (1993) Ascorbate free radical as a marker of oxidative stress: an EPR study. Free Radic Biol Med 14:49–55.

Castronovo V, Scifo P, Castellano A, Aloia MS, Iadanza A, Marelli S, Cappa SF, Strambi LF, Falini A (2014) White matter integrity in obstructive sleep apnea before and after treatment. Sleep 37:1465–1475.

Chang L, Ernst T, Osborn D, Seltzer W, Leonido-Yee M, Poland RE (1998) Proton spectroscopy in myotonic dystrophy: correlations with CTG repeats. Arch Neurol 55:305–311.

Dampney RA, Furlong TM, Horiuchi J, Iigaya K (2013) Role of dorsolateral periaqueductal grey in the coordinated regulation of cardiovascular and respiratory function. Auton Neurosci 175:17–25.

Davis PJ, Zhang SP, Bandler R (1996) Midbrain and medullary regulation of respiration and vocalization. Prog Brain Res 107:315–325.

Demougeot C, Garnier P, Mossiat C, Bertrand N, Giroud M, Beley A, Marie C (2001) N-Acetylaspartate, a marker of both cellular dysfunction and neuronal loss: its relevance to studies of acute brain injury. J Neurochem 77:408–415.

Erecinska M, Silver IA (1990) Metabolism and role of glutamate in mammalian brain. Prog Neurobiol 35:245–296.

Farmer DG, Bautista TG, Jones SE, Stanic D, Dutschmann M (2014) The midbrain periaqueductal grey has no role in the generation of the respiratory motor pattern, but provides command function for the modulation of respiratory activity. Respir Physiol Neurobiol 204:14–20.

Fatouleh RH, Hammam E, Lundblad LC, Macey PM, McKenzie DK, Henderson LA, Macefield VG (2014) Functional and structural changes in the brain associated with the increase in muscle sympathetic nerve activity in obstructive sleep apnoea. Neuroimage Clin 6:275–283.

Faull OK, Jenkinson M, Clare S, Pattinson KT (2015) Functional subdivision of the human periaqueductal grey in respiratory control using 7 tesla fMRI. NeuroImage 113:356–364.

Franklin KA, Lindberg E (2015) Obstructive sleep apnea is a common disorder in the population-a review on the epidemiology of sleep apnea. J Thorac Dis 7:1311–1322.

Fuchs A, Boesiger P, Schulte RF, Henning A (2014) ProFit revisited. Magn Reson Med 71:458–468.

Fung SJ, Xi MC, Zhang JH, Sampogna S, Yamuy J, Morales FR, Chase MH (2007) Apnea promotes glutamate-induced excitotoxicity in hippocampal neurons. Brain Res 1179:42–50.

Gehrmann J, Matsumoto Y, Kreutzberg GW (1995) Microglia: intrinsic immuneffector cell of the brain. Brain Res Brain Res Rev 20:269–287.

Govindaraju V, Young K, Maudsley AA (2000) Proton NMR chemical shifts and coupling constants for brain metabolites. NMR Biomed 13:129–153.

Granziera C, Schmahmann JD, Hadjikhani N, Meyer H, Meuli R, Wedeen V, Krueger G (2009) Diffusion spectrum imaging shows the structural basis of functional cerebellar circuits in the human cerebellum in vivo. PLoS One 4:e5101.

Grebe M, Eisele HJ, Weissmann N, Schaefer C, Tillmanns H, Seeger W, Schulz R (2006) Antioxidant vitamin C improves endothelial function in obstructive sleep apnea. Am J Respir Crit Care Med 173:897–901.

Haddad JJ (2002) Oxygen-sensitive pro-inflammatory cytokines, apoptosis signaling and redox-responsive transcription factors in development and pathophysiology. Cytokines Cell Mol Ther 7:1–14.

Harper RM, Bandler R, Spriggs D, Alger JR (2000) Lateralized and widespread brain activation during transient blood pressure elevation revealed by magnetic resonance imaging. J Comp Neurol 417:195–204.

Harper RM, Gozal D, Bandler R, Spriggs D, Lee J, Alger J (1998) Regional brain activation in humans during respiratory and blood pressure challenges. Clin Exp Pharmacol Physiol 25:483–486.

Harper RM, Macey PM, Henderson LA, Woo MA, Macey KE, Frysinger RC, Alger JR, Nguyen KP, Yan-Go FL (2003) FMRI responses to cold pressor challenges in control and obstructive sleep apnea subjects. J Appl Physiol 94:1583–1595.

Harper RM, Macey PM, Woo MA, Macey KE, Keens TG, Gozal D, Alger JR (2005) Hypercapnic exposure in congenital central hypoventilation syndrome reveals CNS respiratory control mechanisms. J Neurophysiol 93:1647–1658.

Henderson LA, Fatouleh RH, Lundblad LC, McKenzie DK, Macefield VG (2016) Effects of 12 Months Continuous Positive Airway Pressure on Sympathetic Activity Related Brainstem Function and Structure in Obstructive Sleep Apnea. Front Neurosci 10:90.

Hudgel DW, Lamerato LE, Jacobsen GR, Drake CL (2012) Assessment of multiple health risks in a single obstructive sleep apnea population. J Clin Sleep Med 8:9–18.

Jensen JH, Helpern JA, Ramani A, Lu H, Kaczynski K (2005) Diffusional kurtosis imaging: the quantification of non-gaussian water diffusion by means of magnetic resonance imaging. Magn Reson Med 53:1432–1440.

Joo EY, Jeon S, Kim ST, Lee JM, Hong SB (2013) Localized cortical thinning in patients with obstructive sleep apnea syndrome. Sleep 36:1153–1162.

Joo EY, Tae WS, Lee MJ, Kang JW, Park HS, Lee JY, Suh M, Hong SB (2010) Reduced brain gray matter concentration in patients with obstructive sleep apnea syndrome. Sleep 33:235–241.

Kazemi H (2006) Midbrain neurotransmitters in acute hypoxic ventilatory response. Adv Exp Med Biol 580:223–226 [Discussion 351–229].

Kimelberg HK, Goderie SK, Higman S, Pang S, Waniewski RA (1990) Swelling-induced release of glutamate, aspartate, and taurine from astrocyte cultures. J Neurosci 10:1583–1591.

Kizilgoz V, Aydin H, Tatar IG, Hekimoglu B, Ardic S, Firat H, Donmez C (2013) Proton magnetic resonance spectroscopy of periventricular white matter and hippocampus in obstructive sleep apnea patients. Polish J Radiol 78:7–14.

Kumar R, Pham TT, Macey PM, Woo MA, Yan-Go FL, Harper RM (2014) Abnormal myelin and axonal integrity in recently diagnosed patients with obstructive sleep apnea. Sleep 37:723–732.

Kurth F, Zilles K, Fox PT, Laird AR, Eickhoff SB (2010) A link between the systems: functional differentiation and integration within the human insula revealed by meta-analysis. Brain Struct Funct 214:519–534.

Lundblad LC, Fatouleh RH, Hammam E, McKenzie DK, Macefield VG, Henderson LA (2014) Brainstem changes associated with increased muscle sympathetic drive in obstructive sleep apnoea. NeuroImage 103:258–266.

Macey KE, Macey PM, Woo MA, Harper RK, Alger JR, Keens TG, Harper RM (2004) FMRI signal changes in response to forced expiratory loading in congenital central hypoventilation syndrome. J Appl Physiol 97:1897–1907.

Macey KE, Macey PM, Woo MA, Henderson LA, Frysinger RC, Harper RK, Alger JR, Yan-Go F, Harper RM (2006) Inspiratory loading elicits aberrant fMRI signal changes in obstructive sleep apnea. Respir Physiol Neurobiol 151:44–60.

Macey PM, Henderson LA, Macey KE, Alger JR, Frysinger RC, Woo MA, Harper RK, Yan-Go FL, Harper RM (2002) Brain morphology associated with obstructive sleep apnea. Am J Respir Crit Care Med 166:1382–1387.

Macey PM, Kumar R, Woo MA, Valladares EM, Yan-Go FL, Harper RM (2008) Brain structural changes in obstructive sleep apnea. Sleep 31:967–977.

Macey PM, Macey KE, Henderson LA, Alger JR, Frysinger RC, Woo MA, Yan-Go F, Harper RM (2003) Functional magnetic resonance imaging responses to expiratory loading in obstructive sleep apnea. Respir Physiol Neurobiol 138:275–290.

Macey PM, Sarma MK, Nagarajan R, Aysola R, Siegel JM, Harper RM, Thomas MA (2016) Obstructive sleep apnea is associated with low GABA and high glutamate in the insular cortex. J Sleep Res 25:390–394.

Macey PM, Woo MA, Macey KE, Keens TG, Saeed MM, Alger JR, Harper RM (2005) Hypoxia reveals posterior thalamic, cerebellar, midbrain, and limbic deficits in congenital central hypoventilation syndrome. J Appl Physiol 98:958–969.

Meldrum BS (2000) Glutamate as a neurotransmitter in the brain: review of physiology and pathology. J Nutr 130:1007S–1015S.

Moffett JR, Ross B, Arun P, Madhavarao CN, Namboodiri AM (2007) N-Acetylaspartate in the CNS: from neurodiagnostics to neurobiology. Prog Neurobiol 81:89–131.

Ni HF, Zhang JX, Harper RM (1990) Respiratory-related discharge of periaqueductal gray neurons during sleep-waking states. Brain Res 511:319–325.

O'Donoghue FJ, Wellard RM, Rochford PD, Dawson A, Barnes M, Ruehland WR, Jackson ML, Howard ME, Pierce RJ, Jackson GD (2012) Magnetic resonance spectroscopy and neurocognitive dysfunction in obstructive sleep apnea before and after CPAP treatment. Sleep 35:41–48.

Ohnishi T, Tanizawa Y, Watanabe A, Nakamura T, Ohba H, Hirata H, Kaneda C, Iwayama Y, Arimoto T, Watanabe K, Mori I, Yoshikawa T (2013) Human myo-inositol monophosphatase 2 rescues the nematode thermotaxis mutant ttx-7 more efficiently than IMPA1: functional and evolutionary considerations of the two mammalian myo-inositol monophosphatase genes. J Neurochem 124:685–694.

Otake K, Reis DJ, Ruggiero DA (1994) Afferents to the midline thalamus issue collaterals to the nucleus tractus solitarii: an

anatomical basis for thalamic and visceral reflex integration. J Neurosci 14:5694–5707.

Rebec GV, Pierce RC (1994) A vitamin as neuromodulator: ascorbate release into the extracellular fluid of the brain regulates dopaminergic and glutamatergic transmission. Prog Neurobiol 43:537–565.

Sakuma Y, Tada K (1984) Evidence that two sizes of ventromedial hypothalamic neurones project to the mesencephalic central grey matter in rats. J Physiol 349:287–297.

Sarchielli P, Presciutti O, Alberti A, Tarducci R, Gobbi G, Galletti F, Costa C, Eusebi P, Calabresi P (2008) A 1H magnetic resonance spectroscopy study in patients with obstructive sleep apnea. Eur J Neurol 15:1058–1064.

Sarma MK, Macey PM, Nagarajan R, Aysola R, Harper RM, Thomas MA (2016) Accelerated echo planer J-resolved spectroscopic imaging of putamen and thalamus in obstructive sleep apnea. Sci Rep 6.

Sarma MK, Macey PM, Nagarajan R, Aysola R, Harper RM, Thomas MA (2016) Accelerated echo planer J-resolved spectroscopic imaging of putamen and thalamus in obstructive sleep apnea. Sci Rep 6:31747.

Sarma MK, Nagarajan R, Macey PM, Kumar R, Villablanca JP, Furuyama J, Thomas MA (2014) Accelerated echo-planar J-resolved spectroscopic imaging in the human brain using compressed sensing: a pilot validation in obstructive sleep apnea. AJNR Am J Neuroradiol 35:S81–89.

Schuff N, Meyerhoff DJ, Mueller S, Chao L, Sacrey DT, Laxer K, Weiner MW (2006) N-acetylaspartate as a marker of neuronal injury in neurodegenerative disease. Adv Exp Med Biol 576:241–262 [Discussion 361–243].

Schulte RF, Boesiger P (2006) ProFit: two-dimensional prior-knowledge fitting of J-resolved spectra. NMR Biomed 19:255–263.

Shi P, Diez-Freire C, Jun JY, Qi Y, Katovich MJ, Li Q, Sriramula S, Francis J, Sumners C, Raizada MK (2010) Brain microglial cytokines in neurogenic hypertension. Hypertension 56:297–303.

Shinno H, Inagaki T, Miyaoka T, Okazaki S, Kawamukai T, Utani E, Inami Y, Horiguchi J (2007) A decrease in N-acetylaspartate and an increase in myoinositol in the anterior cingulate gyrus are associated with behavioral and psychological symptoms in Alzheimer's disease. J Neurol Sci 260:132–138.

Siesjo BK (1978) Brain energy metabolism and catecholaminergic activity in hypoxia, hypercapnia and ischemia. J Neural Transm Suppl I:17–22.

Siesjo BK, Carlsson C, Hagerdal M, Nordstrom CH (1976) Brain metabolism in the critically ill. Crit Care Med 4:283–294.

Simmons ML, Frondoza CG, Coyle JT (1991) Immunocytochemical localization of N-acetyl-aspartate with monoclonal antibodies. Neuroscience 45:37–45.

Stagg CJ, Rothman DL (2014) Magnetic resonance spectroscopy: tools for neuroscience research and emerging clinical applications. Amsterdam: Elsevier/Academic Press.

Subramanian HH (2013) Descending control of the respiratory neuronal network by the midbrain periaqueductal grey in the rat in vivo. J Physiol 591:109–122.

Subramanian HH, Holstege G (2014) The midbrain periaqueductal gray changes the eupneic respiratory rhythm into a breathing pattern necessary for survival of the individual and of the species. Prog Brain Res 212:351–384.

Szatkowski M, Barbour B, Attwell D (1990) Non-vesicular release of glutamate from glial cells by reversed electrogenic glutamate uptake. Nature 348:443–446.

Thompson RH, Swanson LW (1998) Organization of inputs to the dorsomedial nucleus of the hypothalamus: a reexamination with Fluorogold and PHAL in the rat. Brain Res Brain Res Rev 27:89–118.

Tonon C, Vetrugno R, Lodi R, Gallassi R, Provini F, Iotti S, Plazzi G, Montagna P, Lugaresi E, Barbiroli B (2007) Proton magnetic resonance spectroscopy study of brain metabolism in obstructive sleep apnoea syndrome before and after continuous positive airway pressure treatment. Sleep 30:305–311.

Trelease RB, Sieck GC, Marks JD, Harper RM (1985) Respiratory inhibition induced by transient hypertension during sleep in unrestrained cats. Exp Neurol 90:173–186.

Tummala S, Palomares J, Kang DW, Park B, Woo MA, Harper RM, Kumar R (2016) Global and regional brain non-gaussian diffusion changes in newly diagnosed patients with obstructive sleep apnea. Sleep 39:51–57.

Waites BA, Ackland GL, Noble R, Hanson MA (1996) Red nucleus lesions abolish the biphasic respiratory response to isocapnic hypoxia in decerebrate young rabbits. J Physiol 495(Pt 1):217–225.

Wallace A, Bucks RS (2013) Memory and obstructive sleep apnea: a meta-analysis. Sleep 36:203–220.

Woo MA, Macey PM, Macey KE, Keens TG, Woo MS, Harper RK, Harper RM (2005) FMRI responses to hyperoxia in congenital central hypoventilation syndrome. Pediatr Res 57:510–518.

Xu W, Chi L, Row BW, Xu R, Ke Y, Xu B, Luo C, Kheirandish L, Gozal D, Liu R (2004) Increased oxidative stress is associated with chronic intermittent hypoxia-mediated brain cortical neuronal cell apoptosis in a mouse model of sleep apnea. Neuroscience 126:313–323.

Yadav SK, Kumar R, Macey PM, Richardson HL, Wang DJ, Woo MA, Harper RM (2013) Regional cerebral blood flow alterations in obstructive sleep apnea. Neurosci Lett 555:159–164.

Yadav SK, Kumar R, Macey PM, Woo MA, Yan-Go FL, Harper RM (2014) Insular cortex metabolite changes in obstructive sleep apnea. Sleep 37:951–958.

Yaouhi K, Bertran F, Clochon P, Mezenge F, Denise P, Foret J, Eustache F, Desgranges B (2009) A combined neuropsychological and brain imaging study of obstructive sleep apnea. J Sleep Res 18:36–48.

Yoshimoto M, Miki K, Fink GD, King A, Osborn JW (2010) Chronic angiotensin II infusion causes differential responses in regional sympathetic nerve activity in rats. Hypertension 55:644–651.